Probing the Kinetic Cooperativity of β-Sheet Folding Perpendicular to the Strand Direction†

Yao Xu, Michelle R. Bunagan, Jia Tang, and Feng Gai*

Department of Chemistry, University of Pennsylvania, Philadelphia, Pennsylvania 19104

Received November 2, 2007; Revised Manuscript Received December 10, 2007

ABSTRACT: In an attempt to determine how the folding dynamics of multistranded β-sheets vary with the strand number, we have studied the temperature-induced relaxation kinetics of a four-stranded β-sheet, ^{D}P^{D}P^{D}P. Our results show that the thermally induced relaxation of ^{D}P^{D}P^{D}P occurs on the nanosecond time scale; however, a comparison of the current results with those obtained on a sequence-related, three-stranded β-sheet suggests that increasing the strand number from three to four increases the folding free energy barrier by a minimum of 0.8 kcal/mol, depending on the folding mechanism. Therefore, these results together suggest that the relaxation kinetics of ^{D}P^{D}P^{D}P can be analyzed according to a two-state model even though its folding may actually involve parallel (but degenerate or nearly degenerate) kinetic pathways. The apparent, two-state folding time of ^{D}P^{D}P^{D}P is determined to be ∼0.44 μs at the thermal melting temperature, which makes it one of the fastest folders known to date.

Recently, many studies aimed at providing a molecular understanding of how proteins fold (*1*−*5*) have focused on small, designed peptides in an attempt to extract physical parameters critical to the description of the folding energy landscape of a specific fold or motif (*6*−*19*). The advantage of using designed peptides, capable of folding into a well-defined secondary or tertiary structure, is the ability to systematically vary the sequence content in order to examine the molecular interactions essential for the folding and stability of the targeted fold. For example, our current understanding of the thermodynamic and kinetic determinants of β-hairpin folding largely results from studies on designed peptides (*20*−*31*), since naturally occurring two-stranded β-sheets are usually unstable and/or prone to aggregation in the absence of stabilizing tertiary contacts. Moreover, the use of *de novo* designed β-sheet systems has allowed critical assessment of the effect of strand length and number on the conformational stability of various antiparallel β-sheet motifs (*32*−*36*). In light of these previous thermodynamic studies, it would be quite useful and also interesting to further explore how the folding kinetics of a β-sheet depend on its strand number. Herein, we have studied and compared the temperature jump (*T*-jump) induced relaxation kinetics of two antiparallel β-sheets consisting of three or four strands, in an attempt to elucidate how the folding rate of these β-sheets varies with the number of strands and also to determine if the four-stranded β-sheet shows cooperative folding kinetics.

It has been shown that a β-sheet can exhibit cooperative folding in both parallel (*35*, *37*) and perpendicular directions (*34*, *36*) with respect to the β-strand. For example, using various designed peptide sequences, Gellman and co-workers and Searle and co-workers have shown that within certain limits the stability of a β-sheet increases with increasing strand length (*35*) and strand number (*34*, *36*), indicative of thermodynamic folding cooperativity along these directions. On the other hand, their studies have also indicated that each strand in a multistranded β-sheet could show different thermal melting tendencies (*34*, *36*), suggesting that the folding of these designed β-sheet molecules may involve partially folded intermediate states, distinct steps and/or parallel pathways. Using NMR chemical shift measurements, Andersen and co-workers (*38*) have shown that the thermal unfolding transition of a designed, three-stranded β-sheet, ^{D}P^{D}P (sequence: VFITS^{D}PGKTYTEV^{D}PGOKILQ, where ^{D}P = D-Pro and O = Orn), is indeed consistent with a microscopic folding scheme wherein four conformational states, including the folded, unfolded, and two intermediate states, are involved. Furthermore, their study suggests that the two intermediates lie along parallel folding pathways yet share a similar structure wherein either the C-terminal or N-terminal β-hairpin is folded. This finding, at first glance, seems to contradict our recent study on the folding kinetics of a sequence-related, three-stranded β-sheet, ^{D}P^{D}P-II (sequence: RFIEV^{D}PGKKFITS^{D}PGKTYTE), which shows that the conformational relaxation of this peptide in response to a *T*-jump occurs on the nanosecond time scale and over a single-exponential time course (*39*). However, this apparent discrepancy may be resolved if symmetry is considered.

For many designed, multistranded β-sheet systems, especially the ^{D}P^{D}P series (*36*), the turn and strand sequences are (often) optimized for β-sheet formation, thus resulting in a certain degree of symmetry in their folded topology and consequently in their folding. In other words, the putative parallel pathways involved in the folding of a symmetric, multistranded β-sheet should be degenerate (in both folding thermodynamics and kinetics) (*40*, *41*). Therefore, we suspect that many designed, multistranded β-sheets show simple phenomenological relaxation kinetics even though they fold

† Supported by the National Institutes of Health (Grants GM-065978 and RR-01348).

* To whom correspondence should be addressed. Tel: 215-573-6256. Fax: 215-573-2112. E-mail: gai@sas.upenn.edu.

10.1021/bi702195c CCC: $40.75
Published on Web 01/16/2008

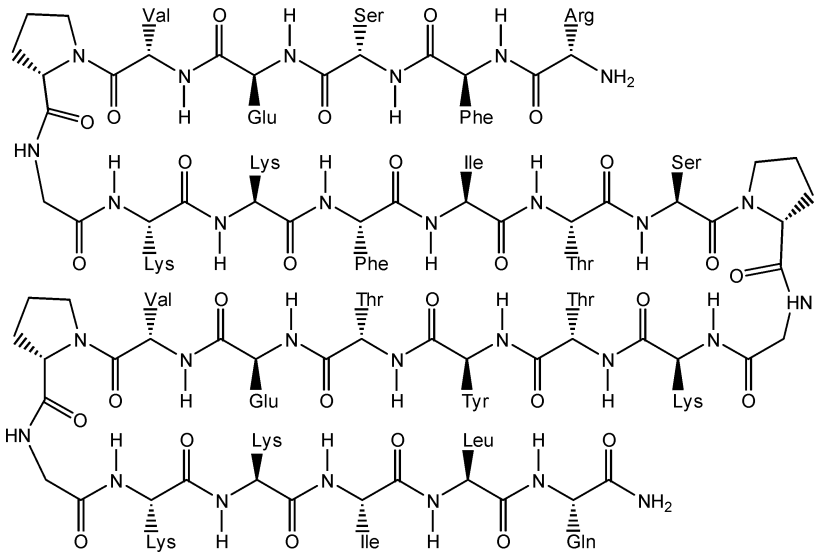

FIGURE 1: Amino acid sequence of $^{D}P^{D}P^{D}P$ with backbone alignment: RFSEV^{D}PGKKFITS^{D}PGKTYTEV^{D}PGKKILQ.

via parallel pathways, provided that these individual pathways are nearly degenerate and also exhibit simple folding kinetics. To verify this hypothesis and to further determine how the folding rate of multistranded β-sheets varies with the number of strands, we have studied the conformational stability and folding kinetics of a 28-residue peptide, named $^{D}P^{D}P^{D}P$, using infrared (IR) spectroscopy. $^{D}P^{D}P^{D}P$ was originally designed by Gellman and co-workers (*36*), who showed that this peptide adopts a four-stranded antiparallel β-sheet structure in aqueous solution. As indicated (Figure 1), $^{D}P^{D}P^{D}P$ is a lengthened version of $^{D}P^{D}P$-II, with eight residues being added at the C-terminus to form an additional β-turn and strand. Therefore, by studying the relaxation kinetics of this four-stranded β-sheet we expect not only to determine if it folds cooperatively but also to determine the apparent increase in the folding free energy barrier associated with the addition of an extra strand to the three-stranded β-sheet $^{D}P^{D}P$-II.

MATERIALS AND METHODS

Materials. $^{D}P^{D}P^{D}P$ was synthesized using standard solid-phase peptide synthesis on Rink resin and purified to homogeneity by reverse-phase HPLC. The identity of the peptide was further verified by matrix-assisted laser desorption ionization mass spectrometry. Subsequently, multiple rounds of lyophilization were carried out in 0.1 M DCl solution to remove the residual trifluoroacetic acid (TFA) from peptide synthesis. For both equilibrium and time-resolved IR studies, the peptide sample was prepared by directly dissolving lyophilized peptide solid in D_2O. The peptide concentration was determined to be ~3 mM using Tyr absorbance at 276 nm. No aggregation was observed under the current experimental conditions.

FTIR Measurement. FTIR spectra were collected on a Magna-IR 860 spectrometer (Nicolet, WI) equipped with a HgCdTe detector using a spectral resolution of 2 cm^{-1}. A home-made, two-compartment, 52 μm CaF_2 sample cell mounted on a programmable translation stage was used to allow separate and alternate measurements of the single-beam spectra of the sample and reference under identical conditions. Temperature control with $\pm$0.2 °C precision was achieved through a thermostated copper block and a temperature bath. The reported spectra correspond to the average of 256 scans.

Infrared T-jump Apparatus. The time-resolved *T*-jump IR apparatus used in the current study has been described in detail elsewhere (*11*). Briefly, a 1.9 μm laser pulse, generated via Raman shifting of the fundamental output of a Q-switched Nd:YAG laser in H_2, was used to generate an 8−10 °C *T*-jump, and the *T*-jump induced transient absorbance change of a sample was measured by a continuous wave (CW) IR diode laser in conjunction with a 50 MHz HgCdTe detector. Digitization of the signal was carried out by a digital oscilloscope. A thermostated, two-compartment sample cell with a 52 μm path length was used to allow separate measurement of the sample and D_2O under identical conditions. The measurements on D_2O provide information for both background subtraction and *T*-jump amplitude determination. The latter was achieved by using the *T*-jump induced absorbance change of D_2O at the probing frequency ν, $\Delta A(\Delta T, \nu)$, and the following equation: $\Delta A(\Delta T, \nu) = a(\nu)*\Delta T + b(\nu)*\Delta T^2$, where ΔT corresponds to the difference between the final (T_f) and initial (T_i) temperatures, and $a(\nu)$ and $b(\nu)$ are constants that were determined by analyzing the temperature dependence of the FTIR spectra of D_2O.

RESULTS AND DISCUSSION

The $^{D}P^{D}P^{D}P$ peptide used in the current study is identical to that designed by Syud *et al.* (*36*), except that the non-natural amino acid ornithine in the original sequence was substituted with lysine. An earlier study has shown that the secondary structural propensity of ornithine is similar to that of lysine (*35*). Therefore, it is expected that such substitution will not result in any significant change in the thermal stability of the folded conformation (*36*). Our previous study on $^{D}P^{D}P$-II indeed corroborated this expectation (*39*).

Equilibrium Study. The thermal unfolding transition of $^{D}P^{D}P^{D}P$ was assessed by monitoring the change of its amide I′ band as a function of temperature (from 1.6 to 88.0 °C with a step of roughly 6 °C). The amide I′ band of polypeptides mainly arises from the stretching vibrations of amide carbonyls and is an established reporter of protein

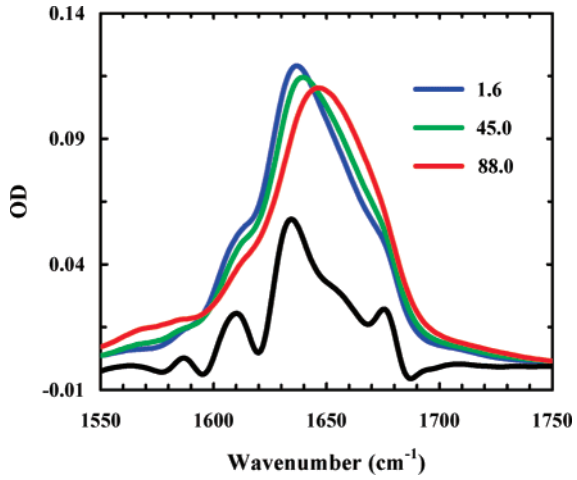

FIGURE 2: Representative FTIR spectra of $^{D}P^{D}P^{D}P$ in D_2O (pH* 4.0) at 1.6, 45.0, 88.0 °C, as indicated. Also shown is the resolution enhanced FTIR spectrum at 1.6 °C (black), which is achieved by Fourier self-deconvolution (FSD) using an enhancement factor of 2 and a bandwidth of 18 cm^{-1}. The FSD spectrum at the amide I′ band of $^{D}P^{D}P^{D}P$ at low temperature consists of four resolvable spectral features, centered at ca. 1612, 1637, 1655, and 1678 cm^{-1}, respectively. The narrow band at 1678 cm^{-1} is characteristic of antiparallel β-sheet structures.

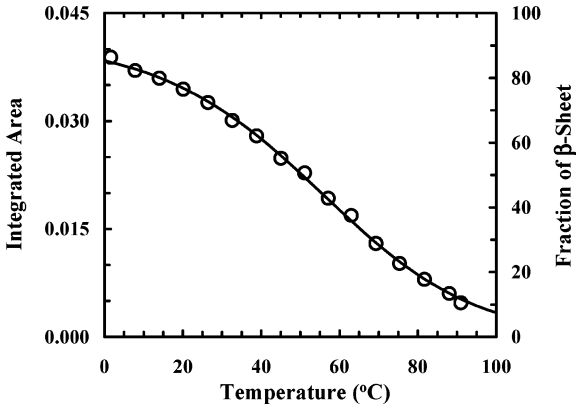

FIGURE 3: Integrated area of the 1678 cm^{-1} band (left *y*-axis) and the fraction of β-sheet (right *y*-axis) versus temperature (open cycles). Fitting these data to a two-state model (solid line) with temperature-independent folded and unfolded baselines yields the following thermodynamic parameters for unfolding: $\Delta H_m = 9.3 \pm 1.2$ kcal mol^{-1}, $\Delta S_m = 28.9 \pm 3.8$ cal mol^{-1} K^{-1}, $\Delta C_p = 121 \pm 25$ cal mol^{-1} K^{-1}, and $T_m = 50.5 \pm 0.8$ °C.

secondary structure content (*42*). As shown (Figure 2), the amide I′ band of $^{D}P^{D}P^{D}P$ at low temperatures is composed of four resolvable spectral features centered at about 1612, 1637, 1655, and 1678 cm^{-1}, respectively. Following Keiderling and co-workers (*24*), we attribute the 1612 cm^{-1} band to the stretching vibration of the amide carbonyl of the D-Pro residues. This assignment is further supported by the fact that the area of this band is estimated to be ~11% of the total area of the amide I′ band of the peptide, which is consistent with the percentage of D-Pro residues in the sequence of $^{D}P^{D}P^{D}P$. The pair of bands centered at about 1637 and 1678 cm^{-1}, on the other hand, is characteristic of antiparallel β-sheets, arising from the unique coupling patterns among amide vibrators in such structures (*43*, *44*). Thus, these IR results corroborate the study of Syud *et al.* (*36*), demonstrating that $^{D}P^{D}P^{D}P$ folds into an antiparallel β-sheet conformation in aqueous solution.

The FTIR difference spectra of $^{D}P^{D}P^{D}P$, obtained by subtracting the spectrum collected at the lowest temperature (i.e., 1.6 °C) from those collected at higher temperatures, indicate that the pair of bands associated with the antiparallel β-sheet structure loses intensity with increasing temperature (data not shown), further demonstrating that they can be used to probe the thermally induced conformational changes of $^{D}P^{D}P^{D}P$. To obtain a quantitative description of the thermal unfolding transition of this β-sheet, we further analyzed these FTIR difference spectra using a global fitting method (*45*), allowing the determination of the temperature dependence of the 1678 cm^{-1} band. As shown (Figure 3), the resultant thermal unfolding transition is broad, indicating that thermodynamically this designed, four-stranded β-sheet folds in a less cooperative manner than many naturally occurring β-sheet proteins. However, we find this transition can still be described by a two-state folding model (Figure 3), revealing that the fractional population of the β-sheet conformation at 4 °C is approximately 84%. This result is in good agreement with that of Syud *et al.* (*36*), who estimated that the population of one hairpin within the four-stranded β-sheet is 75−83%, depending on the residue selected for NMR chemical shift analysis.

Our analysis further shows that the thermal melting temperature (i.e., $T_m = 50.5 \pm 0.8$ °C) of $^{D}P^{D}P^{D}P$ is comparable to that (~52.6 °C) of $^{D}P^{D}P$-II (*39*), suggesting that the enthalpy gain arising from extending the strand number from three to four is well balanced by the concomitant entropy loss. In other words, increasing the strand number to five or larger is unlikely to further increase the conformational stability of the folded state of such designed β-sheet systems. Similarly, it has been shown that increasing the peptide length along the strand direction increases β-hairpin stability, yet the enhancement is saturated at a strand length of 7−9 residues (*35*).

T-Jump Kinetic Study. The folding/unfolding kinetics of $^{D}P^{D}P^{D}P$ were studied by a *T*-jump IR technique, which has been described in detail elsewhere (*11*). Briefly, this technique uses a burst of photons at about 1.9 μm to heat up a D_2O solution within a few nanoseconds. The resultant *T*-jump subsequently induces a population-redistribution among conformational ensembles or substates that are accessible to the molecular system in question and originally at equilibrium. Hence, the time course in which the nonequilibrium state, initially created by the *T*-jump pulse, evolves toward the new equilibrium position determined by the final temperature contains information regarding the kinetics of folding and unfolding. In this study, the *T*-jump induced relaxation kinetics were probed by monitoring the absorbance change at a characteristic frequency (i.e., 1634 cm^{-1}) of β-sheet conformations. Similar to those observed for $^{D}P^{D}P$-II (*39*), the *T*-jump induced relaxation kinetics of $^{D}P^{D}P^{D}P$ consist of two distinct phases (Figure 4). Based on our previous studies (*31*, *46*), the fast phase, which is too fast to be resolved by the current setup, is attributed to temperature-induced spectral changes, such as those arising from temperature-induced dehydration (*46*), as well as imperfect background subtraction. The slow phase is resolvable for final temperatures below 70 °C and is attributed to conformational relaxations between β-sheet and disordered conformations. Interestingly, we find that the slow phase can be adequately modeled by a single-exponential function with a sub-microsecond time constant (Figure 5), suggesting that

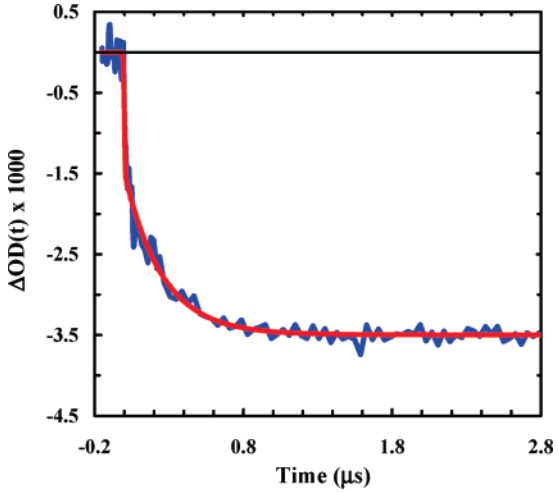

FIGURE 4: A representative relaxation kinetic trace probed at 1633 cm^{-1} for $^{D}P^{D}P^{D}P$ in response to a *T*-jump of 31.6 to 39.1 °C. The smooth line is the fit to the function $OD(t) = A[1 - B*\exp(-t/\tau)]$, with $A = -0.0035$, $B = 0.58$, and $\tau = 253 \pm 25$ ns, convolved with the instrument response function determined from the rise time of the D_2O temperature.

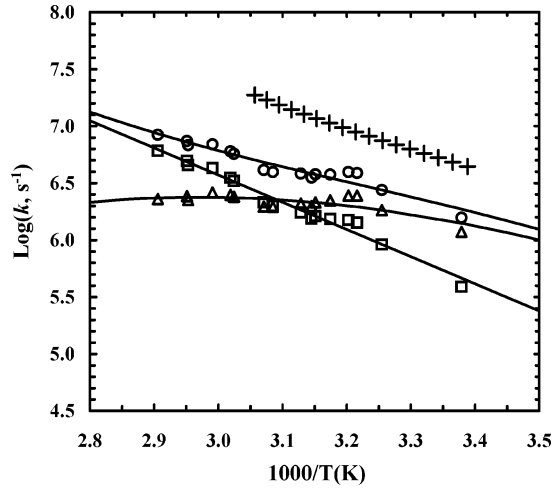

FIGURE 5: Arrhenius plot of the measured relaxation rate constants (○) and also the folding (△) and unfolding (□) rate constants obtained from a two-state analysis. Lines are fits to the Eyring equation. Also shown (+) are the relaxation rate constants for $^{D}P^{D}P$-II (*39*).

the folding of this four-stranded β-sheet is not only kinetically cooperative but also fast. For example, the folding time constant at 50.5 °C is determined to be 0.48 ± 0.08 μs, similar to that observed for protein loop dynamics (*47*).

Due to the reasons discussed below, these kinetic results are both interesting and surprising to some extent. First, despite the fact that $^{D}P^{D}P^{D}P$ folds into a more complex structure, its relaxation rate is similar to that observed for many alanine-based monomeric α-helices (*48*), the folding of which mostly involves local interactions. Second, considering the fact that several segments of $^{D}P^{D}P^{D}P$ (e.g., $^{D}P^{D}P$-II and $^{D}P^{D}P$) can fold independently, and also that multistranded β-sheet folding has been suggested to involve parallel kinetic pathways (*34*, *36*, *38*), one would expect that the conformational relaxation of $^{D}P^{D}P^{D}P$ in response to a *T*-jump should follow non-single-exponential kinetics, provided that these parallel pathways are kinetically distinguishable.

The molecular folding mechanism of $^{D}P^{D}P^{D}P$ is difficult to assess on the basis of this study alone. However, there have been several attempts made in the past to provide a microscopic understanding of the folding mechanism of designed, multistranded β-sheets via computer simulations (*40*, *41*, *49*−*52*). The study of Caflisch and co-workers (*40*, *41*) indicates that the folding of a designed, 20-residue, three-stranded antiparallel β-sheet involves two folding pathways, both involving the almost complete formation of one of the two β-hairpins, followed by consolidation of the unstructured strand. However, their simulations also show that both the folding and unfolding kinetics of this peptide are well described by a single-exponential function. While the simulation of Wang and Sung (*50*) on $^{D}P^{D}P$ indicates an alternative folding mechanism wherein the folding is initiated by fast formation of the turns, followed by a collapse to a compact structure which then finally folds to the native state, their results also demonstrate that the folding kinetics are characterized by one rate-limiting step. Using replica exchange molecular dynamics simulation, Simmerling and co-workers (*53*) further show that although the folding of $^{D}P^{D}P$ involves multiple states, the cooperativity perpendicular to strand direction, which is measured as the degree to which a preformed hairpin reduces the free energy of formation of the other, is about 3 kcal/mol regardless of which hairpin is considered. Taken together, these simulation studies therefore suggest that while the microscopic folding mechanism of designed, multistranded β-sheets could be complex, the overall folding/unfolding kinetics, such as those observed in a *T*-jump IR experiment, may not show significant deviation from simple two-state kinetic behavior. In addition, such designed β-sheet systems often contain optimized turn and stand sequences for β-sheet formation (*36*, *54*). Thus, it is reasonable to assume that any parallel folding pathways involved in such systems are practically degenerate, leading to simpler relaxation kinetics.

Regardless of the microscopic detail of its folding mechanism, the ultrafast relaxation or folding behavior of $^{D}P^{D}P^{D}P$ is consistent with the view that turn formation contributes significantly to the folding free energy barrier of simple β-sheet motifs (e.g., β-hairpin) and that an intrinsically rigid turn can speed up the folding process (*25*, *30*). This is because the three type II′ β-turns connecting the antiparallel β-strands of $^{D}P^{D}P^{D}P$ are formed by D-Pro-Gly (^{D}PG) segments. It has been shown not only that the use of ^{D}PG segments to form two-residue turns between adjacent β-strands promotes β-hairpin formation in shorter peptides (*54*) but also that the intrinsic structural rigidity of the D-Pro residue backbone can constrain the flexibility of the thermally unfolded ensemble (*39*, *55*). Consequently, the conformational space accessible to the thermally unfolded state becomes highly reduced, leading to a rapid conformational relaxation in response to a *T*-jump. Consistent with this argument, our previous study (*39*) shows that the *T*-jump induced conformational relaxation of $^{D}P^{D}P$-II also occurs on the nanosecond time scale. Taken together, these results suggest that both peptides fold on the sub-microsecond time scale as a result of preformed turn structures which bias the thermally unfolded conformation toward the folded state.

Folding Free Energy Barrier. The observation here that the *T*-jump induced population redistribution of $^{D}P^{D}P^{D}P$ follows single-exponential kinetics is consistent with, al-

though not definitive proof of (*56*), kinetic cooperativity of folding along the direction perpendicular to the β-strands. Evidence in support of this picture comes from the fact that the *T*-jump induced relaxation rate of $^{D}P^{D}P$-II is roughly three times that of $^{D}P^{D}P^{D}P$. If the folding of $^{D}P^{D}P^{D}P$ is non-cooperative, within a certain temperature range one would expect to observe a *T*-jump induced relaxation rate that is similar to that observed for $^{D}P^{D}P$-II, corresponding to the folding/unfolding kinetics of a partially folded, three-stranded β-sheet conformation. However, the relaxation rate of $^{D}P^{D}P^{D}P$ is always slower than that of $^{D}P^{D}P$-II over the entire temperature range studied here (Figure 5), thus suggesting that the respective three-stranded β-sheet conformations, as well as other partially folded conformations, are likely only transiently populated. Furthermore, the slower folding kinetics of $^{D}P^{D}P^{D}P$ indicates that adding the fourth strand amplifies the free energy barrier separating the folded from the thermally unfolded states, due to chain connectivity (which allows coupling of local chain motions to motions of other chain segments). Since $^{D}P^{D}P^{D}P$ and $^{D}P^{D}P$-II have similar thermal unfolding temperatures, we can estimate, for temperatures near the midpoint of the thermal unfolding transition, the apparent increase in the folding free energy barrier (i.e., $\Delta\Delta G^{\ddagger}$) due to the increase in peptide chain length, according to the following equation derived based on the transition state theory:

$$\Delta\Delta G^{\ddagger} = -RT \ln\left(\frac{k_{IV}}{k_{III}}\right)$$

where k_{IV} and k_{III} represent the relaxation rates of the four- and three-stranded β-sheets, respectively. At 50 °C, $\Delta\Delta G^{\ddagger}$ is calculated to be about 0.8 kcal/mol using the data presented in Figure 5.

It is worth noting that the interpretation of the above $\Delta\Delta G^{\ddagger}$ value depends on the microscopic folding mechanism of $^{D}P^{D}P^{D}P$. For instance, if the folding of this four-stranded β-sheet involves only one predominant pathway, then the recovered $\Delta\Delta G^{\ddagger}$ value reflects the net increase in the folding free energy barrier. On the other hand, if folding involves two parallel, but nearly degenerate pathways, in which the rate-limiting step corresponds to the formation of either the N-terminal or C-terminal three-stranded β-sheet for example, the net increase in the folding free energy barrier for each path would become 1.4 kcal/mol (0.8 kcal/mol + RT ln(2)), when compared to the folding of $^{D}P^{D}P$-II. While the increase becomes more difficult to estimate if both peptides involve parallel folding pathways, the value of 0.8 kcal/mol nevertheless represents a lower bound. Although the current study does not allow us to determine how many parallel pathways are involved in the folding of $^{D}P^{D}P^{D}P$, the results nonetheless indicate that size is an important determinant of protein folding rates, as observed in simulation and experimental studies (*57*−*60*). Moreover, our results are consistent with studies concerning the effect of additional tails on the kinetics of interior loop formation (*61*−*64*). For example, the study of Fierz and Kiefhaber (*63*) indicates that the formation of type III loops (i.e., interior-to-interior loops) is 1.7-fold slower than formation of type II loops (i.e., end-to-interior loops), whereas the rate of type II loop formation is 2.5-fold slower than the end-to-end collision rate.

While $^{D}P^{D}P^{D}P$ exhibits a very fast relaxation rate in response to a *T*-jump, the above comparative analysis suggests that the folding free energy barrier associated with the individual kinetic pathways is sufficiently large (*65*) that the measured relaxation kinetics can be analyzed according to a two-state model. As shown (Figure 5), such a two-state analysis reveals that the folding rate of $^{D}P^{D}P^{D}P$ is remarkably fast and exhibits only a weak temperature dependence, a feature that has also been observed in computational (*21*, *40*, *41*, *53*) and experimental studies of β-sheet folding (*25*, *30*, *39*). For example, the folding time of $^{D}P^{D}P^{D}P$ at 50 °C is ~0.44 μs, whereas at 25 °C it folds in ~0.67 μs. Given its ultrafast folding rate, small size and complex structure, we believe that $^{D}P^{D}P^{D}P$ represents an interesting yet challenging model system for further computational studies (*66*−*68*).

CONCLUSIONS

De novo designed β-sheets have been widely used to explore factors governing the thermodynamics of β-sheet formation. Here, we further show that the folding kinetics of sequence-related, multistranded β-sheets can be investigated to understand certain features of the folding dynamics of β-sheet motif. Specifically, we have studied the thermal unfolding transition and also *T*-jump induced relaxation kinetics of a designed, four-stranded β-sheet, $^{D}P^{D}P^{D}P$, and compared the results with those obtained previously on a three-stranded β-sheet, $^{D}P^{D}P$-II, in an attempt to elucidate how the folding dynamics vary with the number of strands. Our equilibrium IR results show that the thermal unfolding transition of $^{D}P^{D}P^{D}P$ is broader than that of $^{D}P^{D}P$-II, indicative of a decrease in the thermodynamic folding cooperativity. Furthermore, our time-resolved measurements show that the conformational relaxation of $^{D}P^{D}P^{D}P$ in response to a *T*-jump occurs on the sub-microsecond time scale and follows single-exponential kinetics; however, its relaxation rate is distinctly slower than that of $^{D}P^{D}P$-II. Using a simple comparative analysis, we are able to further show that the addition of the fourth strand increases the folding barrier by a minimum of 0.8 kcal/mol, which underscores the length-dependence (perpendicular to the strand) of the folding rate of multistranded β-sheets. Taken together, these results strongly suggest that the folding of $^{D}P^{D}P^{D}P$ can be described by an apparent two-state model, although its folding may actually involve microscopic parallel, but degenerate pathways.

REFERENCES

1. Bryngelson, J. D., Onuchic, J. N., Socci, N. D., and Wolynes, P. G. (1995) Funnels, pathways, and the energy landscape of protein-folding—A synthesis, *Proteins 21*, 167−195.
2. Chan, H. S., and Dill, K. A. (1998) Protein folding in the landscape perspective: Chevron plots and non-Arrhenius kinetics, *Proteins 30*, 2−33.
3. Daggett, V., and Fersht, A. (2003) The present view of the mechanism of protein folding, *Nat. Rev. Mol. Cell Biol. 4*, 497−502.
4. Dyer, R. B. (2007) Ultrafast and downhill protein folding, *Curr. Opin. Struct. Biol. 17*, 38−47.
5. Dill, K. A., Ozkan, S. B., Weikl, T. R., Chodera, J. D., and Voelz, V. A. (2007) The protein folding problem: when will it be solved, *Curr. Opin. Struct. Biol. 17*, 342−346.
6. Struthers, M. D., Cheng, R. P., and Imperiali, B. (1996) Design of a monomeric 23-residue polypeptide with defined tertiary structure, *Science 271*, 342−345.

7. Cochran, A. G., Skelton, N. J., and Starovasnik, M. A. (2001) Tryptophan zippers: Stable, monomeric beta-hairpins, *Proc. Natl. Acad. Sci. U.S.A. 98*, 5578−5583.
8. Neidigh, J. W., Fesinmeyer, R. M., and Andersen, N. H. (2002) Designing a 20-residue protein, *Nat. Struct. Biol. 9*, 425−430.
9. Chu, R., Takei, J., Knowlton, J. R., Andrykovitch, M., Pei, W. H., Kajava, A. V., Steinbach, P. J., Ji, X. H., and Bai, Y. W. (2002) Redesign of a four-helix bundle protein by phage display coupled with proteolysis and structural characterization by NMR and X-ray crystallography, *J. Mol. Biol. 323*, 253−262.
10. Gillespie, B., Vu, D. M., Shah, P. S., Marshall, S. A., Dyer, R. B., Mayo, S. L., and Plaxco, K. W. (2003) NMR and temperature-jump measurements of de novo designed proteins demonstrate rapid folding in the absence of explicit selection for kinetics, *J. Mol. Biol. 220*, 813−819.
11. Zhu, Y., Alonso, D. O. V., Maki, K., Huang, C. Y., Lahr, S. J., Daggett, V., Roder, H., DeGrado, W. F., and Gai, F. (2003) Ultrafast folding of alpha(3): A de novo designed three-helix bundle protein, *Proc. Natl. Acad. Sci. U.S.A. 100*, 15486−15491.
12. Devi, V. S., Binz, H. K., Stumpp, M. T., Pluckthun, A., Bosshard, H. R., and Jelesarov, I. (2004) Folding of a designed simple ankyrin repeat protein, *Protein Sci. 13*, 2864−2870.
13. Cochran, F. V., Wu, S. P., Wang, W., Nanda, V., Saven, J. G., Therien, M. J., and DeGrado, W. F. (2005) Computational de novo design and characterization of a four-helix bundle protein that selectively binds a nonbiological cofactor, *J. Am. Chem. Soc. 127*, 1346−1347.
14. Nguyen, H., Jäger, M., Kelly, J. W., and Gruebele, M. (2005) Engineering beta-sheet protein toward the folding speed limit, *J. Phys. Chem. B 109*, 15182−15186.
15. Bunagan, M. R., Yang, X., Saven, J. G., and Gai, F. (2006) Ultrafast folding of a computationally designed Trp-cage mutant: Trp(2)-cage, *J. Phys. Chem. B 110*, 3759−3763.
16. Du, D. G., and Gai, F. (2006) Understanding the folding mechanism of an alpha-helical hairpin, *Biochemistry 45*, 13131−13139.
17. Hughes, R. M., and Waters, M. L. (2006) Model systems for beta-hairpins and beta-sheets, *Curr. Opin. Struct. Biol. 16*, 514−524.
18. Watters, A. L., Deka, P., Corrent, C., Callender, D., Varani, G., Sosnick, T., and Baker, D. (2007) The highly cooperative folding of small naturally occurring proteins is likely the result of natural selection, *Cell 128*, 613−624.
19. Religa, T. L., Johnson, C. M., Vu, D. M., Brewer, S. H., Dyer, R. B., and Fersht, A. R. (2007) The helix-turn-helix motif as an ultrafast independently folding domain: The pathway of folding of Engrailed homeodomain, *Proc. Natl. Acad. Sci. U.S.A. 104*, 9272−9277.
20. Muñoz, V., Thompson, P. A., Hofrichter, J., and Eaton, W. A. (1997) Folding dynamics and mechanism of beta-hairpin formation, *Nature 390*, 196−199.
21. Pande, V. S., and Rokhsar, D. S. (1999) Molecular dynamics simulations of unfolding and refolding of a beta-hairpin fragment of protein G, *Proc. Natl. Acad. Sci. U.S.A. 96*, 9062−9067.
22. Klimov, D. K., and Thirumalai, D. (2000) Mechanisms and kinetics of beta-hairpin formation, *Proc. Natl. Acad. Sci. U.S.A. 97*, 2544−2549.
23. Zhou, R. H., Berne, B. J., and Germain, R. (2001) The free energy landscape for beta hairpin folding in explicit water, *Proc. Natl. Acad. Sci. U.S.A. 98*, 14931−14936.
24. Hilario, J., Kubelka, J., and Keiderling, T. A. (2003) Optical spectroscopic investigations of model beta-sheet hairpins in aqueous solution, *J. Am. Chem. Soc. 125*, 7562−7574.
25. Du, D. G., Zhu, Y. J., Huang, C. Y., and Gai, F. (2004) Understanding the key factors that control the rate of beta-hairpin folding, *Proc. Natl. Acad. Sci. U.S.A. 101*, 15915−15920.
26. Chen, R. P. Y., Huang, J. J. T., Chen, H. L., Jan, H., Velusamy, M., Lee, C. T., Fann, W. S., Larsen, R. W., and Chan, S. I. (2004) Measuring the refolding of beta-sheets with different turn sequences on a nanosecond time scale, *Proc. Natl. Acad. Sci. U.S.A. 101*, 7305−7310.
27. Dyer, R. B., Maness, S. J., Peterson, E. S., Franzen, S., Fesinmeyer, R. M., and Andersen, N. H. (2004) The mechanism of beta-hairpin formation, *Biochemistry 43*, 11560−11566.
28. Dyer, R. B., Maness, S. J., Franzen, S., Fesinmeyer, R. M., Olsen, K. A., and Andersen, N. H. (2004) Hairpin folding dynamics: The cold-denatured state is predisposed for rapid refolding, *Biochemistry 44*, 10406−10415.
29. Bolhuis, P. G. (2005) Kinetic pathways of beta-hairpin (un)folding in explicit solvent, *Biophys. J. 88*, 50−61.
30. Du, D. G., Tucker, M. J., and Gai, F. (2006) Understanding the mechanism of beta-hairpin folding via phi-value analysis, *Biochemistry 45*, 2668−2678.
31. Xu, Y., Wang, T., and Gai, F. (2006) Strange temperature dependence of the folding rate of a 16-residue beta-hairpin, *Chem. Phys. 323*, 21−27.
32. Sharman, G. J., and Searle, M. S. (1998) Cooperative interaction between the three strands of a designed antiparallel beta-sheet, *J. Am. Chem. Soc. 120*, 5291−5300.
33. de Alba, E., Santoro, J., Rico, M., and Jimenez, M. A. (1999) De novo design of a monomeric three-stranded antiparallel beta-sheet, *Protein Sci. 8*, 854−865.
34. Griffiths-Jones, S. R., and Searle, M. S. (2000) Structure, folding, and energetics of cooperative interactions between the beta-strands of a de novo designed three-stranded antiparallel beta-sheet peptide, *J. Am. Chem. Soc. 122*, 8350−8356.
35. Stanger, H. E., Syud, F. A., Espinosa, J. F., Giriat, I., Muir, T., and Gellman, S. H. (2001) Length-dependent stability and strand length limits in antiparallel beta-sheet secondary structure, *Proc. Natl. Acad. Sci. U.S.A. 98*, 12015−12020.
36. Syud, F. A., Stanger, H. E., Mortell, H. S., Espinosa, J. F., Fisk, J. D., Fry, C. G., and Gellman, S. H. (2003) Influence of strand number on antiparallel beta-sheet stability in designed three- and four-stranded beta-sheets, *J. Mol. Biol. 326*, 553−568.
37. Guo, C. L., Cheung, M. S., Levine, H., and Kessler, D. A. (2002) Mechanisms of cooperativity underlying sequence-independent beta-sheet formation, *J. Chem. Phys. 116*, 4353−4365.
38. Hudson, F. M., and Andersen, N. H. (2006) Measuring cooperativity in the formation of a three-stranded beta sheet (double hairpin), *Biopolymers 83*, 424−433.
39. Xu, Y., Purkayastha, P., and Gai, F. (2006) Nanosecond folding dynamics of a three-stranded beta-sheet, *J. Am. Chem. Soc. 128*, 15836−15842.
40. Ferrara, P., and Caflisch, A. (2000) Folding simulations of a three-stranded antiparallel beta-sheet peptide, *Proc. Natl. Acad. Sci. U.S.A. 97*, 10780−10785.
41. Cavalli, A., Ferrara, P., and Caflisch, A. (2002) Weak temperature dependence of the free energy surface and folding pathways of structured peptides, *Proteins: Struct., Funct., Genet. 47*, 305−314.
42. Krimm, S., and Bandekar, J. (1986) Vibrational spectroscopy and conformation of peptides, polypeptides, and proteins, *Adv. Protein Chem. 38*, 181−364.
43. Miyazawa, T., and Blout, E. R. (1961) Infrared spectra of polypeptides in various conformations−Amide I and II band, *J. Am. Chem. Soc. 83*, 712−719.
44. Moore, W. H., and Krimm, S. (1975) Transition dipole coupling in amide I modes of beta polypeptides, *Proc. Natl. Acad. Sci. U.S.A. 72*, 4933−4935.
45. Wang, T., Xu, Y., Du, D. G., and Gai, F. (2004) Determining beta-sheet stability by Fourier transform infrared difference spectra, *Biopolymer 75*, 163−172.
46. Mukherjee, S., Chowdhury, P., and Gai, F. (2007) Infrared study of the effect of hydration on the amide I band and aggregation properties of helical peptides, *J. Phys. Chem. B 111*, 4596−4602.
47. Lee, J. C., Lai, B. T., Kozak, J. J., Gray, H. B., and Winkler, J. R. (2007) alpha-Synuclein tertiary contact dynamic, *J. Phys. Chem. B 111*, 2107−2112.
48. Wang, T., Zhu, Y. J., Getahun, Z., Du, D. G., Huang, C. Y., DeGrado, W. F., and Gai, F. (2004) Length dependent helix-coil transition kinetics of nine alanine-based peptides, *J. Phys. Chem. B 108*, 15301−15310.
49. Bursulaya, B. D., and Brooks, C. L., III (1999) Folding free energy surface of a three-stranded beta-sheet protein, *J. Am. Chem. Soc. 121*, 9947−9951.
50. Wang, H. W., and Sung, S. S. (2000) Molecular dynamics simulations of three-strand beta-sheet folding, *J. Am. Chem. Soc. 122*, 1999−2009.
51. Colombo, G., Roccatano, D., and Mark, A. E. (2002) Folding and stability of the three-stranded beta-sheet peptide betanova: Insights from molecular dynamics simulations, *Proteins 46*, 380−392.
52. Cavalli, A., Haberthur, U., Paci, E., and Caflisch, A. (2003) Fast protein folding on downhill energy landscape, *Protein Sci. 12*, 1801−1803.

53. Roe, D. R., Hornak, V., and Simmerling, C. (2005) Folding cooperativity in a three-stranded beta-sheet model, *J. Mol. Biol. 352*, 370−381.
54. Espinosa, J. F., Syud, F. A., and Gellman, S. H. (2002) Analysis of the factors that stabilize a designed two-stranded antiparallel beta-sheet, *Protein Sci. 11*, 1492−1505.
55. Kuznetsov, S. V., Hilario, J., Keiderling, T. A., and Ansari, A. (2003) Spectroscopic studies of structural changes in two beta-sheet-forming peptides show an ensemble of structures that unfold noncooperatively, *Biochemistry 42*, 4321−4332.
56. Sanchez, I. E., and Kiefhaber, T. (2003) Origin of unusual Phi-values in protein folding: Evidence against specific nucleation sites, *J. Mol. Biol. 325*, 367−376.
57. Gutin, A. M., Abkevich, V. I., and Shakhnovich, E. I. (1996) Chain length scaling of protein folding time, *Phys. Rev. Lett. 77*, 5433−5436.
58. Ivankov, D. N., Garbuzynskiy, S. O., Alm, E., Plaxco, K. W., Baker, D., and Finkelstein, A. V. (2003) Contact order revisited: Influence of protein size on the folding rate, *Protein Sci. 12*, 2057−2062.
59. Kouza, M., Li, M. S., O'Brien, E. P., Jr., Hu, C. K., and Thirumalai, D. (2006) Effect of finite size on cooperativity and rates of protein folding, *J. Phys. Chem. A 110*, 671−676.
60. Bunagan, M. R., Cristian, L., DeGrado, W. F., and Gai, F. (2006) Truncation of a cross-linked GCN4-p1 coiled coil leads to ultrafast folding, *Biochemistry 45*, 10981−10986.
61. Perico, A., and Beggiato, M. (1990) Intramolecular diffusion-controlled reactions in polymers in the optimized Rouse-Zimm approach. 1. The effect of chain stiffness, reactive site positions, and site numbers, *Macromolecules 23*, 797−803.
62. Ortiz-Repiso, M., Freire, J. J., and Rey, A. (1998) Intramolecular reaction rates of flexible polymers. 1. Simulation results and the classical theory, *Macromolecules 31*, 8356−8362.
63. Fierz, B., and Kiefhaber, T. (2007) End-to-end vs interior loop formation kinetics in unfolded polypeptide chains, *J. Am. Chem. Soc. 129*, 672−679.
64. Doucet, D., Roitberg, A., and Hagen, S. J. (2007) Kinetics of internal-loop formation in polypeptide chains: A simulation study, *Biophys. J. 92*, 2281−2289.
65. Naganathan, A. N., Doshi, U., and Muñoz, V. (2007) Protein folding kinetics: Barrier effects in chemical and thermal denaturation experiments, *J. Am. Chem. Soc. 129*, 5673−5682.
66. Lei, H., Wu, C., Liu, H. G., and Duan, Y. (2007) Folding free-energy landscape of villin headpiece subdomain from molecular dynamics simulations, *Proc. Natl. Acad. Sci. U.S.A. 104*, 4925−4930.
67. Ghosh, K., Ozkan, S. B., and Dill, K. A. (2007) The ultimate speed limit to protein folding is conformational searching, *J. Am. Chem. Soc. 129*, 11920−11927.
68. Ensign, D. L., Kasson, P. M., and Vijay, Pande, S., V. S. (2007) Heterogeneity even at the speed limit of folding: Large-scale molecular dynamics study of a fast-folding variant of the villin headpiece, *J. Mol. Biol. 374*, 806−816.

BI702195C